Environ. Sci. Technol. **2006**, *40,* 1644−1649

Rates of Oxidative Coupling of Humic Phenolic Monomers Catalyzed by a Biomimetic Iron-Porphyrin

DANIELA ŠMEJKALOVÁ† AND ALESSANDRO PICCOLO*,‡

Institute of Physical and Applied Chemistry, Faculty of Chemistry, Brno University of Technology, Purkynova 118, 61200 Brno, Czech Republic, and Dipartimento di Scienze del Suolo, della Pianta e dell'Ambiente, Università di Napoli Federico II, Via Università, 100, 80055 Portici, Italy

A synthetic water-soluble meso-tetra(2,6-dichloro-3-sulfonatophenyl)porphyrinate of iron(III) chloride (FeP) was used as biomimetic catalyst in the oxidative coupling of three monomeric phenols (catechol, caffeic, and *p*-coumaric acids), which are common constituents of natural humic substances. The extent of oxidation induced by the FeP catalyst in solutions of phenolic monomers was followed in the presence of an oxygen donor such as hydrogen peroxide or dissolved oxygen under daylight radiation. Both UV- and fluorescence-detected liquid chromatograms indicated that primary oxidation products had a larger electronic conjugation and molecular mass than the original phenols, thereby suggesting that the biomimetic oxidative catalysis produced covalently linked phenylene and oxyphenylene oligomers. However, the polyphenolic products were further oxidized in the progress of the catalytic reaction to possible undetectable aliphatic acids or even to complete mineralization. Rate constants describing the initial reaction period were larger for the catalyzed oxidation with hydrogen peroxide than those for the noncatalyzed control solutions under autoxidation or hydrogen peroxide treatment. However, the rate constants measured for the phenol solutions treated with just the FeP catalyst showed that the presence of dissolved oxygen and the action of the daylight radiation were sufficient to significantly increase the reaction rate in respect to control solutions. These results confirmed previous findings, showing that humic materials may undergo oxidative coupling catalyzed by metal-porphyrins in the presence of either an oxygen donor or, simply, dissolved molecular oxygen under daylight. The increase of molecular mass of natural humic and polyphenolic substances by this biomimetic technology may have useful applications in environmental chemistry.

Introduction

Humic substances (HS) are naturally occurring biomolecules, ubiquitous in water, soil, and sediments. HS in soil compose up to 80% of the organic carbon, while their content in freshwaters may reach about 40−60% of the dissolved organic carbon (DOC) (*1*). The quantity and reactivity of HS in the biosphere amply justifies the intense research on their chemical and biochemical transformation.

A body of experimental evidence recently indicated that natural humic matter can be considered as a supramolecular self-association of heterogeneous molecules that have average mass lower than 1000−2000 Da (*2*−*5*) and are held together, in apparently large sizes, by dispersive forces such as $\pi-\pi$, CH-π, and van der Waals interactions (*6*, *7*). The loosely bound supramolecular associations were found to polymerize into more rigid conformations when subjected to oxidative coupling by enzymatic catalysis with peroxidase (*8*−*10*). The polymerization was attributed to a number of phenolic monomers present in the humic suprastructures that are known to undergo oxidative coupling reactions when catalyzed by oxidative enzymes and produce polyphenols consisting of covalently linked phenylene and oxyphenylene units (*11*−*14*).

The catalytic activity of oxidative enzymes may well be mimicked by suitable synthetic metal-porphyrin rings since the reactivity is due to the essential role of the iron-porphyrin system as the active prosthetic group of the enzyme (*15*). A synthetic iron-porphyrin (FeP), a nontoxic compound, has been applied to dechlorinate and oxidatively couple chlorophenols (*16*, *17*) and other organic compounds (*18*, *19*). It is believed that the mechanism of action of iron-porphyrins is induced by an oxygen donor through the formation of a high-valent iron-oxo species. This becomes the active oxidant of phenolic moieties (*15*) that undergo, as in the case of enzyme-catalyzed oxidations (*20*), further couplings via a radical mechanism (*21*). While much work elucidated the role of electronic and structural properties of metal-porphyrins in different biomimetic catalyses (*22*−*25*), little attention has been paid to the mechanisms and rates of oxidative couplings of reactive phenolic constituents of humic substances under the biomimetic catalysis of water-soluble metal-porphyrins.

Humic substances were reported to positively influence the FeP biomimetic catalysis in the oxidative degradation of pentachlorophenol (*26*). A water-soluble FeP was found to catalyze the direct polymerization of humic substances when hydrogen peroxide was the oxygen donor (*27*). However, polymerization of humic substances by metal-porphyrin catalysis also occurred under electromagnetic radiation even without the presence of hydrogen peroxide, thereby suggesting that dissolved oxygen alone may act as oxidant species in the photooxidative coupling of humic components (*28*). This finding agrees with the reported photocatalytic oxidation of synthetic metal-porphyrins on hydrocarbons, such as alkanes and alkenes, with the sole presence of dioxygen (*29*, *30*).

The aim of this work was to verify the catalytic effect of a water-soluble FeP on the oxidative coupling of monomeric phenol molecules, such as catechol, caffeic, and *p*-coumaric acids (Figure 1), which are known to be some of the aromatic constituents of humic substances (*1*, *5*). The FeP catalysis, in either oxidation with hydrogen peroxide or photooxidation with dissolved O_2, was studied by following the disappearance of the selected monomeric phenols and by comparing the rate constants of the oxidation reactions.

Experimental Procedures

Biomimetic Iron-Porphyrin. Information on the synthesis, structure, and characterization of the water-soluble meso-tetra-(2,6-dichloro-3-sulfonatophenyl)-porphyrinate of

* Corresponding author e-mail: alpiccol@unina.it.
† Brno University of Technology.
‡ Università di Napoli Federico II.

10.1021/es051760i CCC: $33.50

Published on Web 01/25/2006

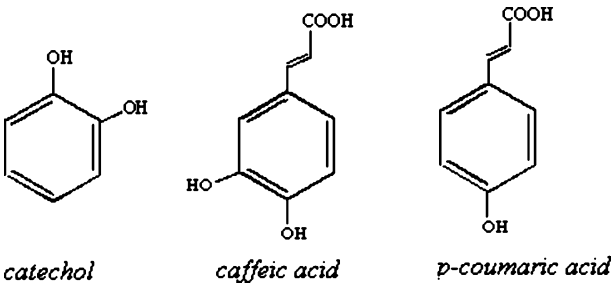

catechol *caffeic acid* *p-coumaric acid*

FIGURE 1. Structures of the monomeric phenols.

Fe(III) [Fe(TDCPPS)Cl] used here as a biomimetic catalyst are reported elsewhere (*27*, *28*).

Humic Phenolic Monomers. 1,2-Benzenediol or catechol (C), 3-(3,4-dihydroxyphenyl)acrylic acid or trans-caffeic acid (TCA) and 3-(4-hydroxyphenyl)acrylic acid or trans *p*-coumaric acid (TPCA) were purchased by Sigma-Aldrich (Germany), with purity ranging between 97 and 99%. All phenolic monomers were used without further purification.

Reaction Solutions. The control solutions containing only the separate substrate (S) of C (0.45 mM), TCA (0.28 mM), and TPCA (0.30 mM) were obtained by dissolving each phenol in methanol and MilliQ grade water (Millipore) to a final methanol−water ratio of approximately 1:99 (v/v). A second set of solutions (S + H_2O_2) consisted in an aliquot (25 mL) of each control phenol solution added with 117 μL of a 0.017 M solution of hydrogen peroxide (Ashland Chemical, Italy) to reach a final concentration of 0.08 mM in hydrogen peroxide. A third set of solutions (S + FeP) was made by adding, to each control phenol solution (25 mL), 2.75, 5.50, and 8.25 mL of a 1.09×10^{-4} M solution of the FeP catalyst, thereby reaching a final concentration of 12, 24, and 36 μM in FeP, respectively. A fourth set of solutions (S + FeP + H_2O_2) was similarly treated with FeP but further added with 117 μL of a 0.017 M solution of hydrogen peroxide. A mixed solution containing three phenols together was prepared with a final concentration of 0.45, 0.28, and 0.30 mM in C, TCA, and TPCA, respectively. The mixed solution was further made either 12 μM in FeP alone or, additionally, 0.08 mM in hydrogen peroxide.

All solutions were prepared in triplicate, added with 1.0 μL of toluene (Sigma-Aldrich, Germany; 97% purity) as a bacteriostatic agent, and filtered through a 0.45 μm Millipore filter. The progress of the oxidative coupling of phenols under different catalytic conditions was followed by reverse-phase HPLC analysis in a time course of 10 days. During this period, the samples were kept, at room temperature, in stopped volumetric flasks and exposed to daylight without stirring.

HPLC Analysis. A Perkin-Elmer LC 200 pump equipped with a 10 μL loop on a 7125 Rheodyne Rotary Injector, a SPHERI-5 ODS column (220 mm × 4.6 mm, 5 μm, Brownlee) held at a constant temperature of 30 °C, and two detectors in a series (a Perkin-Elmer LS-3B fluorescence spectrometer and a Perkin-Elmer LC-295 UV detector) were used to follow the disappearance of phenols under different conditions. The UV detector was set at 280 nm, whereas the excitation/emission wavelengths set on the fluorescence detector were 278:360, 262:426, 260:422, and 265:405 nm for the chromatography of C, TCA, TPCA, and mixed solutions, respectively.

The chromatography eluent consisted in a binary phase made of acetonitrile (A) and a 0.75% trifluoroacetic acid solution in water (v/v) (B) and was pumped at 1.2 mL min^{-1} in a gradient mode that varied with solutions. In the case of the C solution, A was held for 1 min at 2%, increased to 15% in 10 min, and to 50% in 20 min. This composition was held for 5 min. For both TCA and TPCA solutions, the eluent A was held for 7 min at 2%, increased to 15% in 28 min, to 50% in 20 min, and finally held at 50% for 5 min. In the case of the mixed solution, eluent A was kept at 2% for 7 min, raised to 15% in 33 min, 50% in 28 min, and then held at 50% for 5 min. A Perkin-Elmer TotalChrom 6.2.0 software was employed for the acquisition and evaluation of chromatograms. Quantitative analysis was achieved by calibration curves based on known concentrations of C, TCA, and TPCA solutions in the range of 1−100 mg L^{-1}. All HPLC analyses were conducted in duplicate.

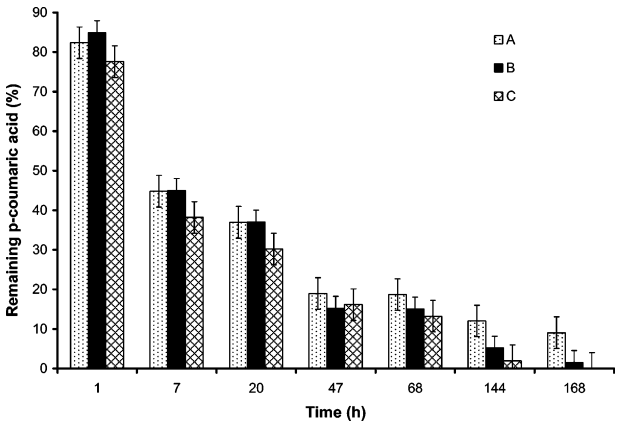

FIGURE 2. Percent modification of *p*-coumaric acid with reaction time and as a function of three different concentrations of the FeP catalyst: A = 12 μM; B = 24 μM; and C = 36 μM.

Results and Discussion

Effect of Catalyst Concentration. The extent of an FeP-catalyzed oxidative coupling reaction may be affected by the amount of FeP that catalyzes the radical oxidation of the substrate and by the nature of the oxygen donor that initiates the radical reaction. The more concentrated the catalyst, the larger the number of active sites participating to the reaction and the amount of phenol derivatives undergoing oxidative couplings.

To evaluate the effect of the FeP concentration on the oxidative reaction of phenolic monomers, hydrogen peroxide was used as oxygen donor. Figure 2 shows (as an example of phenolic behavior) the decrease of TPCA concentration with time in the presence of three different concentrations of the FeP catalyst. Within one week of reaction time, no significant differences in the oxidative degradation of TPCA were observed at the three FeP concentrations. Regardless of FeP concentration, about 20% of the substrate was transformed after 1 h from reaction start, while 20, 47, and 144 h of reaction time lowered the concentration of TPCA by 65, 86, and 96% of the initial value, respectively. The behavior of C and TCA (not shown) was similar to that of TPCA. In fact, about 50% of the initial concentration of C and TCA disappeared after 100 and 50 h from reaction start, while 95 and 97% disappeared after 216 and 192 h, respectively. Because of the comparable effect of the three FeP concentrations on the transformation of substrates, the lowest concentration of iron-porphyrin (12 μM) was employed to further study reaction rates.

Oxidative Coupling Reactions. Coupling reactions between phenolic monomers are catalyzed by an FeP high-valent iron-oxo π cation radical that abstracts a hydrogen from a phenolic substrate (*15*, *20*). The oxo species are directly formed on FeP in the presence of monooxygen donors, such as hydrogen peroxide. However, formation of Fe(IV)═O porphyrin π cation radicals can be induced also in the presence of dissolved triplet oxygen, by trapping molecular oxygen on reduced metallic Fe(II)P center. Reduction of a metal-porphyrin can be achieved by heating or irradiating a porphyrin solution under light of wavelength >390 nm (*31*).

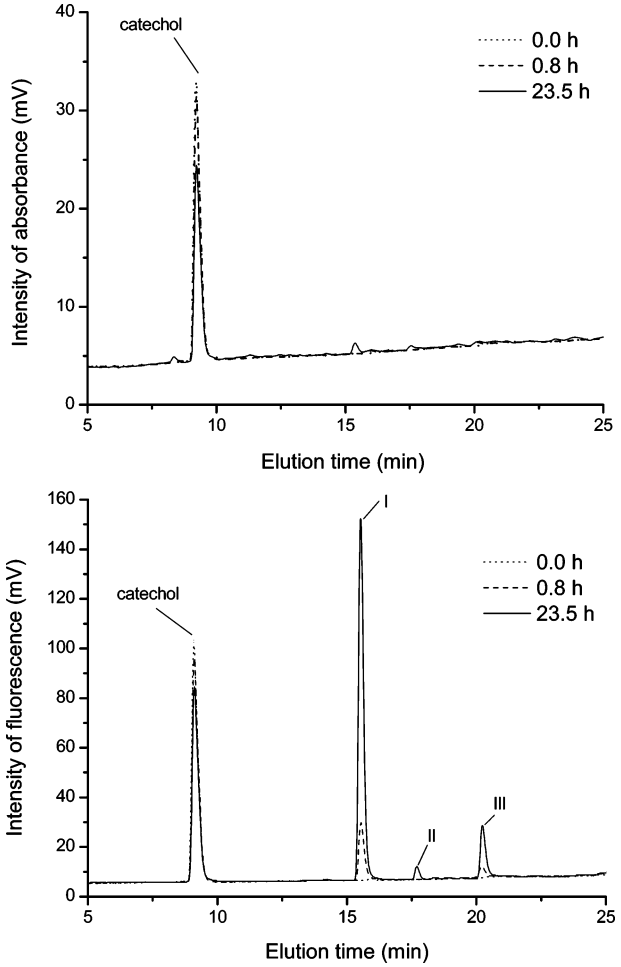

FIGURE 3. UV (upper) and fluorescence (lower) detected chromatograms of catechol added with both FeP and H_2O_2 at different reaction times: 0, 0.8, and 23.5 h. Peaks representing reaction products are labeled I−III.

Both H_2O_2 as oxygen donor and dissolved molecular oxygen were earlier proposed to be involved in the FeP-catalyzed coupling of humic components (*27*, *28*). To verify the role played by the oxidant, the selected phenol constituents of humic molecules were subjected to the oxidative coupling reaction, both with and without the presence of H_2O_2, in either separate or mixed solutions. The possibility of a reduction of the metallic center was enabled by exposing the reaction solutions to daylight. Reaction behavior and oxidation products were followed by liquid chromatography coupled to fluorescence and UV detectors. We found that the same oxidation products were formed from substrates regardless of the presence of H_2O_2.

Figure 3 reports both UV- and fluorescence-detected chromatograms of the separate C solution. The catalytic oxidation of C did not reveal any change in the UV-detected chromatograms, except for a significant decrease of the original substrate. However, the fluorescence-detected chromatogram of the same solution showed peaks of reaction products I−III, which increased in intensity up to about 24 h (Figure 3) and then began to decline steadily. Peaks I and III were also observed, although of lower intensity, in the chromatogram of the noncatalyzed C solution (unshown). Therefore, the oxidation reaction of C occurs to some extent in aqueous solution, and it is accelerated in the presence of the biomimetic catalyst. The occurrence of product II only in the catalyzed system suggests that a different oxidation mechanism takes place in each case. The appearance and then the decline of peaks I−III for the catalyzed C solution suggest that they represent unstable intermediate products of reaction and are susceptible to further oxidation.

Some oxidation products of C, such as pyrogallol (1,2,3-trihydroxybenzene), ring-opening fragments, quinones, C dimers, and hydroxybenzaldehydes, have been reported in the literature for the catalysis with TiO_2 (*32*, *33*). In the present study, the peaks for reaction products of C oxidation eluted at larger elution times than C itself (Figure 3), thereby implying a less polar structure than the original substrate. This consideration leads to exclusion of the rather polar pyrogallol as a possible oxidation product. C dimers or aliphatic ring-opening fragments may be both susceptible to a later elution from the chromatographic column due to either a larger mass or increased hydrophobic adsorption on the stationary phase. However, aliphatic fragments derived from an oxidative ring-opening of C would hardly possess sufficient conjugated groups to allow fluorescence detection. Thus, a dimeric structure appears to be the most probable result of an FeP catalyzed oxidation of C. In fact, peak I was the only product for which the formation of a C dimer through carbon−carbon coupling was confirmed by GC/MS analysis (for experimental details and C dimer mass spectrum, see Supporting Information). Other reaction products found here were not obtained in sufficient amounts or were not stable enough for a successful purification followed by GC/MS analysis.

The oxidative coupling of separate TCA produced two reaction products (not shown). Since the same products were observed also for the oxidation of TCA in the mixed solution, they can be seen as peaks I and II in the UV-detected chromatogram of Figure 4. Both peaks reached a maximum intensity after 5 days from reaction start and thereafter steadily declined, thereby suggesting that they were intermediates of further oxidation reactions. Except for the decrease of the initial TCA concentration, no other changes were observed by either UV or fluorescence detection. Studies on the enzymatic oxidation of TCA reported the formation of an *o*-quinone of caffeic acid [3-(3′,4′-dioxo-1′,5′-cyclohexadienyl)propenoic acid] that may undergo further coupling reactions and form dimers (*34*). This *o*-quinone and some of the possible caffeic acid dimers were reported to be detectable at the 280 nm wavelength used here (*35*).

On the basis of the results from the TPCA separate solution (not shown), peak III in the UV-detected chromatogram of the mixed solution (Figure 4) was attributed to a reaction product of TPCA oxidation. This peak reached its maximum intensity after 3 days from reaction start and then began to decrease. Since this intermediate was eluted just before the original TPCA molecule, it is likely to possess a polar structure similar to that of TPCA, most probably a quinone or an isomer of this. Except for the formation of peak III and the decrease of the initial TPCA concentration, there were no other changes observed by either UV or fluorescence detection for catalytic oxidation of separate TPCA solution. A TPCA oxidation catalyzed by sodium periodate, which is claimed (*35*) to yield the same products as those observed for catalysis by phenoloxidases, was reported to produce only trace amounts of 4-hydroxybenzenaldehyde (*35*). A Fenton reaction (an inorganic source of OH radicals) applied to TPCA and followed by liquid chromatography was found to produce degradation intermediates such as *p*-vinyl phenol, 3,4-dihydroxybenzaldehyde, and oxaloacetic acid (*36*, *37*).

The UV-detected chromatogram of the mixed solution (Figure 4) revealed that the reacting substrates had an elution time that was in order of decreasing polarity (C < TCA < TPCA) and generally reflected the elution times of the phenols in the respective separate solutions. Besides the original monomeric phenols, the chromatograms revealed peaks I−III that were previously observed and described each monomeric phenol as a separate substrate in solution. Figure 4 also shows that the same oxidation products were observable in the UV

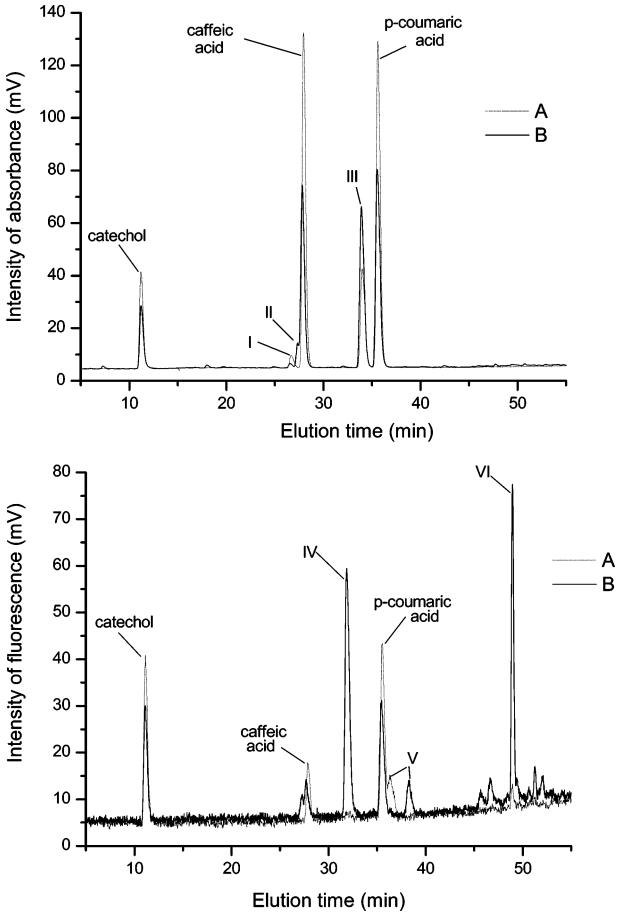

FIGURE 4. Liquid chromatograms of the mixed solution of three phenols revealed by UV (upper) and fluorescence (lower) detectors. (A) Mixed solution added with H_2O_2 (S + H_2O_2). (B) Same solution as in panel A, but added with the FeP catalyst (S + FeP + H_2O_2). Reaction products were labeled I−VI. The chromatograms were recorded after 5 days from the start of the oxidation reaction.

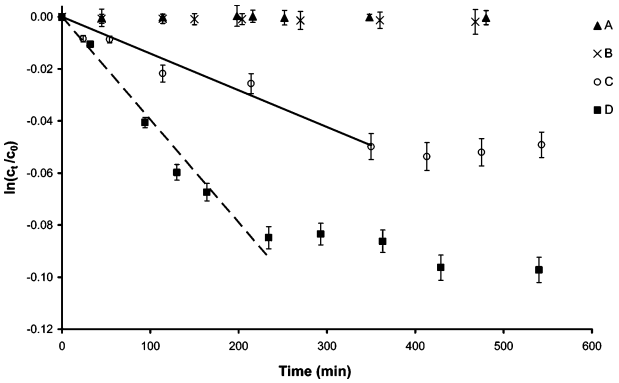

FIGURE 5. Decrease of phenol concentration with time for (A) catechol alone (S); (B) catechol added with H_2O_2 (S + H_2O_2); (C) catechol added with FeP (S + FeP); and (D) catechol added with FeP and H_2O_2 (S + FeP + H_2O_2). Initial rate constants for FeP catalysis were calculated from the slopes of the linear of curves C and D.

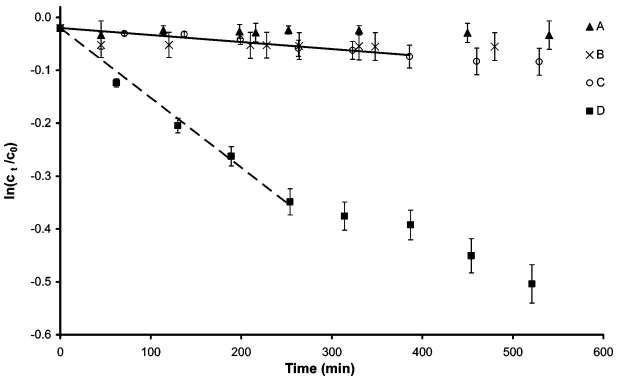

FIGURE 6. Decrease of phenol concentration with time for (A) caffeic acid alone (S); (B) caffeic acid added with H_2O_2 (S + H_2O_2); (C) caffeic acid added with FeP (S + FeP); and (D) caffeic acid added with FeP and H_2O_2 (S + FeP + H_2O_2). Initial rate constants for FeP catalysis were calculated from the slopes of the linear of curves C and D.

chromatograms regardless of the presence of the FeP catalyst. However, the unreacted original substrates appeared to remain twice as intense in the noncatalyzed solution, indicating that the oxidative reaction was significantly more extensive in the presence of the FeP catalyst.

Three further oxidation products (IV−VI) of the catalyzed mixed solution were noted in the fluorescence-detected chromatogram (Figure 4). These peaks reached maximum intensity after 3−5 days from the reaction start and then began to decrease, thereby indicating their further oxidation. However, only peak V was found for both the catalyzed and the noncatalyzed mixed solution. These results suggest that reaction products under peak IV and VI occurred through a reaction pathway that did not take place without the presence of the FeP catalyst. Furthermore, possible products of phenol oxidative coupling may be represented by larger molecules, such as dimers and trimers, eluting later than their monomeric substrates and possessing bond conjugations large enough to make them visible by fluorescence spectroscopy. Thus, the new peaks detected by fluorescence at larger elution times than the monomeric phenols may well be some oligomers formed during the oxidative couplings catalyzed by FeP.

Finally, the reported observation of intermediate reaction products, which first increase and then decline, is in line with chromatographic findings on the oxidation of ferulic acid [3-(4-hydroxy-3-methoxyphenyl)acrylic acid] catalyzed by lignin-peroxidase (*38*). In that case, further incubation of the substrate resulted in the disappearance of peaks identified as dehydro di- or trimers of ferulic acid. In our study, it would then be possible that early products of catalyzed oxidation were the coupled oligomers of the monomeric phenols, which were further oxidized into no longer detectable fragments.

Rate Behavior of Catalyzed Phenol Oxidations. The rate behavior related to the catalyzed oxidation of phenols appeared too complex to allow a suitable approximation to fit all measured data (Figure 2). In fact, the rate of disappearance of original substrates, when either in separate or in mixed solution, began to slow after the first 300−500 min from the start of the reaction (Figures 5−7). The complexity of the oxidation reaction may be attributed to the observed secondary oxidations of intermediate reaction products. Moreover, a decrease of the oxidative reaction rate may be also caused by either decomposition of the oxygen donor, or depletion of dissolved dioxygen, or inactivation of the FeP catalyst.

To overcome the possible factors of decreasing reaction rate, only the initial reaction period was used here to compare the reactivity of the selected humic phenolic monomers under the different oxidation conditions. The initial reaction period was fitted according to the first-order rate equation

$$\ln\frac{c_t}{c_0} = -kt$$

where c_0 and c_t (mol dm^{-3}) represent the concentration of the substrate in solution, at the reaction time 0 and t (min), respectively, and k (min^{-1}) represents the first-order rate constant.

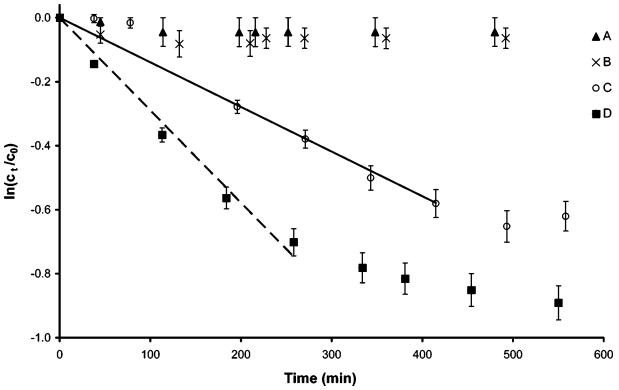

FIGURE 7. Decrease of phenol concentration with time for (A) *p*-coumaric acid alone (S); (B) *p*-coumaric acid added with H_2O_2 (S + H_2O_2); (C) *p*-coumaric acid added with FeP (S + FeP); and (D) *p*-coumaric acid added with FeP and H_2O_2 (S + FeP + H_2O_2). Initial rate constants for FeP catalysis were calculated from the slopes of the linear of curves C and D.

TABLE 1. Initial First-Order Rate Constants, k (min^{-1}), for the Oxidation of Humic Phenolic Monomers (S) as in a Separate (I) or in a Mixture Solution (M) under Different Conditions[a]

phenol (S)	I/M	$k \times 10^{-4}$ (min^{-1}) ± SD			
		S	S + H_2O_2	S + FeP	S + FeP + H_2O_2
C	I	<0.01	0.04 ± 0.01	1.41 ± 0.07	3.95 ± 0.11
	M	<0.08	<0.03	2.39 ± 0.13	2.94 ± 0.09
TCA	I	<0.26	<1.07	1.33 ± 0.05	13.21 ± 0.15
	M	0.80 ± 0.07	<1.15	3.88 ± 0.24	7.28 ± 0.25
TPCA	I	<1.6	<2.09	13.95 ± 0.14	28.93 ± 0.05
	M	3.96 ± 0.25	5.54 ± 0.30	6.02 ± 0.27	5.53 ± 0.15

[a] SD = standard deviation; C = catechol; TCA = trans-caffeic acid; TPCA = trans-*p*-coumaric acid.

The initial first-order rate constants were implied by the straight lines ($R^2 > 0.95$) obtained by plotting ln (c_t/c_0) as a function of reaction time (Figures 5−7). Although the reaction rate behavior appears complex already at the initial stage, the first-order rate constants were considered to be sufficient enough for comparing the reactivities of substrates (*39*).

The calculated first-order rate constants for the different reaction conditions are summarized in Table 1. C showed a larger resistance to autoxidation than TCA and TPCA, when in control conditions (S) for either separate or mixed solutions. The fastest rate of autoxidation ($k = 3.96 \times 10^{-4}\ min^{-1}$) was found for TPCA when in mixed solution. Addition of hydrogen peroxide to the control solutions led to an increased rate of oxidation for all substrates. However, the order of oxidation rate remained unchanged: C ≪ TCA < TPCA.

The presence of the FeP catalyst in the phenol solutions (S + FeP), as either separate or mixed ones, produced a significant acceleration of the oxidation reaction for all substrates (Table 1). The rate of catalyzed oxidation for separate substrates increased in the order C = TCA ≪ TPCA, whereas in the mixed solution it changed to C < TCA < TPCA. However, the rate constants measured for C and TCA in the mixed solutions were much greater than those found for the same constituents when in separate solutions. The opposite was observed for TPCA that gave a significantly larger constant in separate than in mixed solutions.

The oxidation reaction rates (Table 1) increased significantly for the solutions in which the addition of the FeP catalyst was followed by that of hydrogen peroxide (S + FeP + H_2O_2). The values of rate constants reached 3.95×10^{-4}, 13.21×10^{-4}, and $28.93 \times 10^{-4}\ min^{-1}$ for the separate solutions of C, TCA, and TPCA, respectively. The rate constants also increased significantly for the oxidative catalysis of phenols in mixed solution, although to a lower extent than for the separate solutions. An exception was for TPCA, whose rate constant in the mixed solution resulted significantly lower than that found in the presence of FeP alone. This finding can be explained by a possible competition among the single substrates for the oxidation by the high-valent iron-oxo porphyrin π cation radicals. Because of the preference of C and TCA substrates over TPCA, it appears that the FeP high-valent radicals preferentially induce oxidation of molecules possessing more protonated electron-donor groups on the ring, such as the dihydroxybenzenes. Similarly, the different electronic distribution in the structure of the three phenols may easily explain the rest of the observed differences in oxidation reactivity. In particular, the concomitant presence of a hydroxyl and an acrylic group in the TCPA ring appeared to favor the formation of radical species when TPCA was subjected to oxidative catalysis in separate solution. Conversely, in mixed solution, the presence of two hydroxyl groups on the ring seemed to increase the competitive reactivity of TCA, probably through the formation of stable *o*-quinone intermediates, over that of TPCA.

The reaction rates shown in Table 1 also indicated that while the presence of the oxygen donor increased substantially the velocity of catalytic oxidation in the separate solutions, the oxidation in the mixed solution for each phenol compound was at best, as in the case of TCA, hardly twice as intense as that found without H_2O_2. These findings thus suggest that a water-soluble FeP biomimetic catalyst is capable to significantly enhance the oxidation of mixtures of phenols, as in humic solutions, without the need of an additional oxidant but with the sole presence of dissolved oxygen and assistance by the electromagnetic radiation of daylight.

Our results indicate that a synthetic water-soluble iron porphyrin catalyzes the oxidation of phenolic compounds as those present in natural humic solutions, inasmuch as it is observed for enzymatic catalysis. Although the effect of biomimetic catalysis significantly increased in the presence of an oxygen donor such as hydrogen peroxide, we have shown that the catalytic oxidation of phenols had a considerable efficiency even in the sole presence of dissolved dioxygen under exposure to daylight radiation. Moreover, the oxidative catalysis by FeP induced the formation of reaction products that were not observed during autoxidation or oxidation by H_2O_2. In fact, although TCA and TCPA were oxidized faster than C when in separate solutions, the competition among these phenolic compounds in the mixed solution revealed that the active form of FeP preferentially oxidized the substrates having more electron donor groups on the aromatic ring.

The chromatographic profiles of primary oxidation products as detected by fluorescence suggested a larger electronic conjugation and, thus, a larger molecular mass than the original phenolic substrates. This observation is in line with previous literature findings that indicated that phenolic monomers are coupled into larger oligomers under oxidative catalysis. All primary reaction products slowly disappeared with the time course of the catalytic oxidation, after having reached a maximum concentration at an earlier stage. Such a phenomenon was explained with either a progressive oxidative coupling into larger oligomers undetectable at the set HPLC conditions or the ring-opening of primary reaction products. A similar progressive oxidation to aliphatic acids was earlier observed for chlorophenols when subjected to oxidative coupling catalyzed by iron porphyrin (*21*).

This work has confirmed that humic phenolic monomers may rapidly undergo oxidative coupling in the presence of a biomimetic iron-porphyrin catalysts and thus contribute to an increased conformational stability of natural organic matter. In the case of humus, the formation of micellar

suprastructures with the numerous other heterogeneous compounds may prevent further oxidation of the coupling products (*5*, *6*). Moreover, it has been shown here that the oxidative formation of polyphenols from humic phenolic monomers may be induced by the iron-porphyrin catalyst with only the presence of dissolved oxygen under daylight radiation. This result may become significant if advanced chemical technologies are to be employed for the remediation and the protection of the environment.

Acknowledgments

This work was partially supported by a grant from the Assessorato alla Ricerca Scientifica della Regione Campania. D.S. gratefully acknowledges the fellowship received within this grant to conduct research in Portici.

Supporting Information Available

Experimental details on HPLC isolation of an oxidation product, GC/MS analysis, and molecular structures. This material is available free of charge via the Internet at http://pubs.acs.org.

Literature Cited

(1) Kordel, W.; Dassenakis, M.; Lintelmann, J.; Padberg, S. The importance of natural organic material for environmental processes in waters and soils. *Pure Appl. Chem.* **1997**, *69*, 1571−1600.

(2) Piccolo, A. The supramolecular structure of humic substances. *Soil Sci.* **2001**, *166*, 810−833.

(3) Simpson, A. J. Determining the molecular weight, aggregation, structures, and interactions of natural organic matter using diffusion ordered spectroscopy. *Magn. Reson. Chem.* **2002**, *40*, S72−S82.

(4) Piccolo, A.; Spiteller, M. Electrospray ionization mass spectrometry of terrestrial humic substances and their size fractions. *Anal. Bioanal. Chem.* **2003**, *377*, 1047−1059.

(5) Wershaw, R. L. Evaluation of conceptual models of natural organic matter (Humus) from a consideration of the chemical and biochemical processes of humification. U.S. Geological Survey Science Investigative Reports 2004-5121: Reston, VA, 2004.

(6) Piccolo, A. The supramolecular structure of humic substances: A novel understanding of humus chemistry and implications in soil science. *Adv. Agron.* **2002**, *75*, 57−134.

(7) Peuravuori, J. NMR spectroscopy study of freshwater humic material in light of supramolecular assembly. *Environ. Sci. Technol.* **2005**, *39*, 5541−5549.

(8) Piccolo, A.; Conte, P.; Cozzolino, A. Polymerization of humic substances by an enzyme-catalyzed oxidative coupling. *Naturwissenschaften* **2000**, *87*, 391−394.

(9) Cozzolino, A.; Piccolo, A. Polymerization of dissolved humic substances catalyzed by peroxidase. Effects of pH and humic composition. *Org. Geochem.* **2002**, *33*, 281−294.

(10) Weber, W. J., Jr.; Huang, Q.; Pinto, A. Reduction and disinfection byproduct formation by molecular reconfiguration of the fulvic constituents of natural background organic matter. *Environ. Sci. Technol.* **2005**, *39*, 6446−6452.

(11) Kurioka, H.; Komatsu, I.; Uyama, H.; Kobayashi, S. Enzymatic oxidative polymerization of alkylphenols. *Macromol. Rapid Commun.* **1994**, *15*, 507−510.

(12) Wang, P.; Martin, B. D.; Parida, S.; Rethwisch, D. G.; Dordick, J. S. Multienzymic synthesis of poly(hydroquinone) for use as a redox polymer. *J. Am. Chem. Soc.* **1995**, *117*, 12885−12886.

(13) Wang, P.; Dordick, J. S. Enzymatic synthesis of unique thymidine-containing polyphenols. *Macromolecules* **1998**, *31*, 941−943.

(14) Oguchi, T.; Tawaki, H.; Uyama, S.-i.; Kobayashi, S. Soluble polyphenol. *Macromol. Rapid Commun.* **1999**, *20*, 401−403.

(15) Sheldon, R. A. Oxidations catalysis by metalloporphyrins. In *Metalloporphyrins in Catalytic Oxidations*; Sheldon, R. A., Ed.; Dekker: New York, 1994.

(16) Labat, G.; Seris J.-L.; Meunier B. Oxidative degradation of aromatic pollutants by chemical models of ligninase based on porphyrin complexes. *Angew. Chem., Int. Ed. Engl.* **1990**, *29*, 1471−1473.

(17) Chen, S.-T.; Stevens, D. K.; Kang, G. Pentachlorophenol and crystal violet degradation in water and soils using heme and hydrogen peroxide. *Water Res.* **1999**, *33*, 3657−3665.

(18) Traylor, P. S.; Dolphin, D.; Traylor, T. G. Sterically protected hemins with electronegative substituents: efficient catalysts for hydroxylation and epoxidation. *J. Chem. Soc., Chem. Commun.* **1984**, 279−280.

(19) Song, R.; Sorokin, A.; Bernardou, J.; Meunier, B. Metalloporphyrin-catalyzed oxidation of 2-methylnaphthalene to vitamin k_3 and 6-methyl-1,4-naphthoquinone by potassium monopersulfate in aqueous solution. *J. Org. Chem.* **1997**, *62*, 673−678.

(20) Peralta-Zamora, P.; Pereira, C. M.; Tiburtius, E. R. L.; Moraes, S. G.; Rosa, M. A.; Minussi, R. C.; Duraìn, N. Decolorization of reactive dyes by immobilized laccase. *Appl. Catal., B* **2003**, *42*, 131−144.

(21) Meunier, B.; Sorokin, A. Oxidation of pollutants catalyzed by metallophthalocyanines. *Acc. Chem. Res.* **1997**, *30*, 470−476.

(22) Maldotti, A.; Amadelli, R.; Bartocci, C.; Carassiti, V.; Polo, E.; Varani, G. Photochemistry of iron porphyrin complexes. *Coord. Chem. Rev.* **1993**, *125*, 143−154.

(23) Maldotti, A.; Molinari, A.; Andreotti, L.; Fogagnolo, M.; Amadelli, R. Novel reactivity of photoexcited iron porphyrins caged into a polyfluorosulfonated membrane in catalytic hydrocarbon oxygenation. *Chem. Commun.* **1998**, 507−508.

(24) Larson, R. A.; Cervini-Silva, J. Dechlorination of substituted trichloromethanes by an iron(II)porphyrin. *Environ. Toxicol. Chem.* **2000**, *19*, 543−548.

(25) Shimanovich, R.; Groves, J. T. Mechanisms of peroxynitrite decomposition catalyzed by FeTMPS, a bioactive sulfonated iron porphyrin. *Arch. Biochem. Biophys.* **2001**, *387*, 307−317.

(26) Fukushima, M.; Sawada, A.; Kawasaki, M.; Ichikawa, H.; Morimoto, K.; Tatsumi, K.; Aoyama, M. Influence of humic substances on the removal of pentachlorophenol by a biomimetic catalytic system with a water-soluble iron(III)porphyrin complex. *Environ. Sci. Technol.* **2003**, *37*, 1031−1036.

(27) Piccolo, A.; Conte, P.; Tagliatesta, P. Increased conformational rigidity of humic substances by oxidative biomimetic catalysis. *Biomacromolecules* **2005**, *6*, 351−358.

(28) Šmejkalová, D.; Piccolo, A. Enhanced molecular dimensions of a humic acid induced by photooxidation catalyzed by biomimetic metalporphyrins. *Biomacromolecules* **2005**, *6*, 2120−2125.

(29) Weber, L.; Hommel, R.; Behling, J.; Haufe, G.; Hennig, H. Photocatalytic oxygenation of hydrocarbons with (tetraarylporphyrinato)iron(III)complexes and molecular oxygen. Comparison with microsomal cytochrome P-450 mediated oxygenation reactions. *J. Am. Chem. Soc.* **1994**, *116*, 2400−2408.

(30) Maldotti, A.; Molinari, A.; Amadelli, R. Photocatalysis with organized systems for the oxofunctionalization of hydrocarbons by O_2. *Chem. Rev.* **2002**, *102*, 3811−3836.

(31) Gilbert, B. C.; Hodges, G. R.; Smith, J. R. L.; MacFaul, P.; Taylor, P. The photoreactions of the carboxylate complexes of 5,10-, 15-, and 20-tetra(2-*N*-methylpyridyl)porphyrin. *J. Mol. Catal.* **1997**, *117*, 249−257.

(32) Chen, J.; Eberlein, L.; Langford, C. H. Pathways of phenol and benzene photooxidation using TiO_2 supported on zeolite. *J. Photochem. Photobiol., A* **2002**, *148*, 183−189.

(33) Peiró, A. M.; Ayllón, J. A.; Peral, J.; Doménech, X. TiO_2-photocatalyzed degradation of phenol and ortho-substituted phenolic compounds. *Appl. Catal., B* **2001**, *30*, 359−373.

(34) Tazaki, H.; Taguchi, D.; Hayashida, T.; Nabeta, K. Stable isotope-labeling studies on the oxidative coupling of caffeic acid via *o*-quinone. *Biosci. Biotechnol. Biochem.* **2001**, *65*, 2613−2621.

(35) Antolovich, M.; Bedgood, D. R., Jr.; Bishop, A. G.; Jardine, D.; Prenaler, P. D.; Robards, K. LC-MS investigation of oxidation products of phenolic antioxidants. *J. Agric. Food Chem.* **2004**, *52*, 962−971.

(36) Herrea, F.; Pulgarin, C.; Nadtochenko, V.; Kiwi, J. Accelerated photooxidation of concentrated *p*-coumaric acid in homogeneous solution. Mechanistic studies, intermediates, and precursors formed in the dark. *Appl. Catal., B* **1998**, *17*, 141−156.

(37) Gernjak, W.; Krutzler, T.; Glaser, A.; Malato, S.; Caceres, J.; Bauer, R.; Fernandéz-Alba, A. R. Photofenton treatment of water containing natural phenolic pollutants. *Chemosphere* **2003**, *50*, 71−78.

(38) Ward, G.; Hadar, Y.; Bilkis, I.; Konstantinovsky, L.; Dosoretz, C. Initial steps of ferulic acid polymerization by lignin peroxidase. *J. Biol. Chem.* **2001**, *276*, 18734−18741.

(39) Miranda, M. A.; Marin, M. L.; Amat, A. M.; Arques, A.; Seguí, S. Pyrylium salt-photosensitized degradation of phenolic contaminants present in olive oil wastewater with solar light Part III. Tyrosol and *p*-hydroxyphenylacetic acid. *Appl. Catal., B* **2002**, *35*, 167−174.

Received for review September 5, 2005. Revised manuscript received November 21, 2005. Accepted December 19, 2005.

ES051760I